HHS Public Access

Author manuscript

Mol Genet Metab. Author manuscript; available in PMC 2022 December 01.

Published in final edited form as:

Mol Genet Metab. 2021 December ; 134(4): 330–336. doi:10.1016/j.ymgme.2021.11.008.

Reduction of Glutamate Neurotoxicity: A Novel Therapeutic Approach for Niemann-Pick disease, type C1

Antony Cougnoux[1], **Julia C. Yerger**[1,†], **Mason Fellmeth**[1,†], **Jenny Serra-Vinardell**[2], **Fatemeh Navid**[3], **Christopher A. Wassif**[1], **Niamh X. Cawley**[1], **Forbes D. Porter**[1,*]

[1]Division of Translational Medicine, *Eunice Kennedy Shriver* National Institute of Child Health and Human Development, National Institutes of Health, Bethesda, MD, USA

[2]Human Biochemical Genetics Section, National Human Genome Research Institute, National Institutes of Health, Bethesda, MD, USA

[3]Pediatric Translational Research Branch, National Institute of Arthritis and Musculoskeletal and Skin Disease, National Institutes of Health, Bethesda, MD, USA

Abstract

Niemann-Pick disease, type C1 is a progressive, lethal, neurodegenerative disorder due to endolysosomal storage of unesterified cholesterol. Cerebellar ataxia, as a result of progressive loss of cerebellar Purkinje neurons, is a major symptom of Nieman-Pick disease, type C1. Comparing single cell RNAseq data from control (*Npc1*$^{+/+}$) and mutant (*Npc1*$^{-/-}$) mice, we observed significantly decreased expression of *Slc1a3* in *Npc1*$^{-/-}$ astrocytes. *Slc1a3* encodes a glutamate transporter (GLAST, EAAT1) which functions to decrease glutamate concentrations in the post synaptic space after neuronal firing. Glutamate is an excitatory neurotransmitter and elevated extracellular levels of glutamate can be neurotoxic. Impaired EAAT1 function underlies type-6 episodic ataxia, a rare disorder with progressive cerebellar dysfunction, thus suggesting that impaired glutamate uptake in Niemann-Pick disease, type C1 could contribute to disease progression. We now show that decreased expression of *Slc1a3* in *Npc1*$^{-/-}$ mice has functional consequences that include decreased surface protein expression and decreased glutamate uptake by *Npc1*$^{-/-}$ astrocytes. To test whether glutamate neurotoxicity plays a role in Niemann-Pick disease, type C1 progression, we treated NPC1 deficient mice with ceftriaxone and riluzole. Ceftriaxone is a β-lactam antibiotic that is known to upregulate the expression of *Slc1a2*, an alternative glial

*Corresponding Author, Forbes D. Porter, MD, PhD, 10 CRC, Rm. 5-2752, 10 Center Dr., Bethesda, MD 20897, 301-435-4432, fdporter@mail.nih.gov.

†Equal contribution

Author Contributions

AC and FDP designed and initiated the project. AC, JY, MF, JS-V, FN, CAW and NXC conducted or facilitated the experiments. AC, JY and FDP analyzed the Data. AC and JY drafted the initial manuscript and assembled the figures. FDP obtained funding, provided supervision, and wrote the final draft. All authors reviewed, provided input, and approved the manuscript.

Declarations

Mouse experiments were approved by the NICHD Animal Care and Use Committee. All data generated or analyzed during this study are included in the published article and supplementary information files. The authors declare that they have no financial or non-financial competing interests.

glutamate transporter. Although ceftriaxone increased *Slc1a2* expression, we did not observe a treatment effect in NPC1 mutant mice. Riluzole is a glutamate receptor antagonist that inhibits postsynaptic glutamate receptor signaling and reduces the release of glutamate. We found that treatment with riluzole increased median survival in $Npc1^{-/-}$ by 12%. Given that riluzole is an approved drug for the treatment of amyotrophic lateral sclerosis, repurposing of this drug may provide a novel therapeutic approach to decrease disease progression in Niemann-Pick disease type, C1 patients.

Keywords

Niemann-Pick disease; type C1; NPC1; Lysosomal Disease; Glutamate-mediated Neurotoxicity; Purkinje Neurons; Riluzole; SLC1A3; EAAT1; GLAST

Introduction

Niemann-Pick disease, type C (NPC) is a rare, lethal lysosomal disease clinically characterized by progressive neurodegeneration. NPC can be caused by mutation of either *NPC1* or *NPC2*; however, most cases are due to impaired NPC1 function [1]. The incidence of NPC1 is estimated to be on the order of 1/100,000–120,000 [1, 2]. The NPC1 protein, in conjunction with NPC2, transports unesterified cholesterol out of the lysosomal lumen to the lysosomal limiting membrane where it becomes bioavailable [3]. Impaired function of either NPC1 or NPC2 results in endolysosomal accumulation of unesterified cholesterol and decreased cholesterol bioavailability for cellular functions. Major clinical symptoms observed in NPC1 are progressive cerebellar ataxia and dementia [4]. The age of onset is heterogeneous, but NPC1 primarily affects children and adolescents with a median age of death of 13 years [5]. Long-term treatment data has shown that miglustat, a glycosphingolipid synthesis inhibitor, delays NPC1 neurological disease progression and increases survival [6–8]. Although miglustat has been approved for treatment of NPC by the European Medicines Agency and other countries, it is not approved in the United States. Currently there are no FDA approved therapies for NPC1, thus there remains a significant unmet medical need for therapeutic interventions to treat patients with NPC1.

Loss of cerebellar Purkinje neurons underlies the progressive cerebellar ataxia that is observed in NPC1 patients. Purkinje neurons integrate extensive excitatory cerebellar neuronal inputs and are the sole output of the cerebellar cortex, via inhibitory GABAergic signaling, to coordinate motor function. Purkinje neurons show differential sensitivity to loss of NPC1 function with aldolase C positive cells being more resistant to loss [9]. Aldolase C positive Purkinje neurons are enriched in posterior lobules and lateral stripes. A characteristic histopathological finding in NPC1 mice is an anterior to posterior progression of Purkinje neuron loss [10, 11]. The pathological mechanisms underlying the differential sensitivity are not known; however, Purkinje neurons are highly susceptible to glutamate-mediated excitotoxicity [12, 13]. Glutamate is an excitatory neurotransmitter and after synaptic release, extracellular glutamate concentrations are decreased by sodium-dependent plasma membrane glutamate transporters (Excitatory Amino Acid Transporters or EAATs). EAAT1 (GLAST) is encoded by *SLC1A3* and EAAT4 is encoded by *SLC1A6.* These

glutamate transporters function to maintain low extracellular glutamate levels and play a major role in protecting Purkinje neurons from glutamate-mediated excitotoxicity. In the cerebellum, *SLC1A3* is expressed uniformly by glial cells including both Bergmann and radial glia which are closely associated with the soma of Purkinje neurons [14]. *SLC1A6* is expressed by Purkinje neurons, with higher *SLC1A6* expression in aldolase C positive Purkinje neurons [12, 15]. Glutamate hyperstimulation leads to increase calcium influx, mitochondrial dysfunction and unregulated activation of degradative enzymes that ultimately results in cell death [16, 17].

EAAT1 functions as the primary glutamate transporter in the cerebellum and is expressed by astrocytes [18, 19]. Using single cell transcriptome analysis, we recently observed decreased expression of *Slc1a3* in cerebellar astrocytes from NPC1 mutant mice [20] and previous work by Rabenstein *et al.* [21] showed decreased EAAT1 protein expression in cerebellar tissue from NPC1 mutant mice. Loss of EAAT1 function results in type-6 episodic ataxia [22] and glutamate-mediated neurotoxicity has been proposed to contribute to neurodegeneration in common disorders such as Alzheimer disease and Amyotrophic Lateral Sclerosis [23]. We thus hypothesized that glutamate-mediated neurotoxicity could contribute to Purkinje neuron loss and that therapies designed to reduce glutamate toxicity would have potential benefit in the treatment of NPC1. In this paper we further characterized EAAT1 dysfunction in NPC1 and explored the therapeutic potential of reducing glutamate-mediated neurotoxicity.

Materials and Methods

Mouse models and phenotypic evaluation

Mouse experiments were approved by the NICHD Animal Care and Use Committee. BALB/cNctr-Npc1^{m1N}/J (*Npc1*$^{+/-}$) [24] mice were obtained from The Jackson Laboratory (Bar Harbor, ME, USA). Heterozygous *Npc1*$^{+/-}$ mice were intercrossed to obtain control (*Npc1*$^{+/+}$) and mutant (*Npc1*$^{-/-}$) littermates. Mice were genotyped by PCR using ear punch DNA and primers listed in Table S1. Water and chow were available ad libitum. An *a priori* power calculation was performed to guide adequate design of the survival experiment. The mean survival of Balb/c *Npc1*$^{-/-}$ mice in our colony is 75 ± 4 days. Assuming no change in the experimental control mean and standard deviation (*e.g.* due to the vehicle or genetic background) and a similar standard deviation in the experimental group we have 95% power to detect an 8–9 day (~12%) increase in survival at p=0.05 using cohorts of 6–8 mice. Additional mice are enrolled to account for experimental variation and to allow for post-hoc determination of gender differences. A humane survival endpoint was defined as hunched posture, reluctance to move, inability to remain upright when moving and weight loss >30% of peak weight. Ledge test, grooming, motor coordination, kyphosis, and hind limb clasping were assessed as previously described [25]. Individuals conducting the phenotypic assessments were blinded as to treatment status.

Investigational drug administration and sample collection

Riluzole (Selleckchem, Houston, TX, USA) was resuspended in DMSO at 30mg.ml^{-1} as a 500-fold concentrated stock solution and further diluted in drinking water. Water was

replaced every three days. Ceftriaxone (Cayman Chemical, Ann Arbor, MI, USA) was resuspended in PBS at 100 $mg.ml^{-1}$ and a 100 $mg.kg^{-1}$ dose was administered daily by intraperitoneal injection. Dosing of investigational agents was initiated after weaning of the animals on day of life ~21. Six mice per group were sacrificed at 7 weeks of age for pathology and RNA extraction, the remaining animals were treated until they reached the humane disease end point described above. Mutant, control, treated and untreated animals were enrolled concurrently, and efforts were made to balance sex distribution.

Cell culture and glutamate uptake

Cell lines, growth conditions and TaqMan Probes are listed in Table S1. Glutamate concentrations in astrocyte culture media were measured using a fluorometric glutamate assay kit (MET-5080, CellBiolabs, San Diego, USA). Media containing 50μM glutamate was added to the cells and aliquots were collected at 0, 1, 3 and 6 hours for measurement of glutamate concentration. The data represents the percent glutamate remaining in the media after each time point normalized to the initial glutamate concentration. Glutamate uptake was considered to be the difference between initial and remaining concentration of glutamate in the culture medium. Results were normalized to the mean uptake by *Npc1*$^{+/+}$ astrocytes.

Human tissue

Anonymous post-mortem tissue was obtained from the NICHD Blood and Tissue Bank (http://medschool.umaryland.edu/btbank/) and processed for western blot analysis as previously described [26]. Tissue reference numbers are listed in Table S1.

RNA extraction and qPCR

Total RNA was extracted from frozen cell pellets or cerebellar tissue using TRIzol (Thermo Fischer Scientific, Waltham, MA, USA), followed by RNA purification using Qiagen RNeasy Mini Columns (Qiagen, Hilden, Germany). For gene expression analysis by real-time qPCR, the quality and the quantity of RNA was assessed using a NanoDrop (Thermo Fischer Scientific, Waltham, MA, USA). One microgram of total RNA was reverse-transcribed to obtain cDNA using a High-Capacity cDNA Archive Kit, according to the manufacturer's instructions (Thermo Fischer Scientific, Waltham, MA, USA). TaqMan assays used are listed in Table S1 and were used according to the manufacturer's instructions. Amplifications were performed in 96-well plates with an Applied Biosystems 7300 real-time PCR system (Carlsbad, CA, USA). Each sample was analyzed in duplicate, using 50ng of total cDNA per reaction.

Immunofluorescence and Flow Cytometry analysis

Mice were euthanized at 7 weeks by CO_2 asphyxiation and transcardially perfused with 30 ml of PBS, pH 7.4. Brain tissue was further post-fixed in 4% paraformaldehyde solution for 24 hours and then cryoprotected in 30% sucrose (Sigma-Aldrich Millipore, St Louis, MO, USA). Frozen parasagittal sections (20μm) of cerebellar tissue were obtained using a cryostat and then floated in PBS with 0.25% Triton X-100 (Sigma-Aldrich Millipore, St Louis, MO, USA). The tissue sections were stained at 4°C overnight with the antibody and

dyes listed in Table S1. Images were taken using a Zeiss Axio Observer Z1 microscope fitted with an automated scanning stage, Colibri II LED illumination and Zeiss ZEN2 software using a high-resolution AxioCam MRm camera and a 20× objective. Each fluorophore channel was pseudo-colored in ZEN2, exported as a .czi file, and analyzed using ImageJ [27]. Antibodies and working dilutions are listed in Table S1. We have previously described in detail the gating strategy and cell preparation for FACS analysis of mice cerebella [26]. Mean Fluorescence Intensities (MFI) were determined using FlowJo software v9 (TreeStar, Ashland, OR, USA). Histopathological quantification was adapted from our previous work [28]. In ImageJ, GFAP and CD68 density used the "moments" thresholding method at 95% for the measurement performed on manually drawn cerebellar area. Purkinje cells were counted manually by counting the number of calbindin positive cell bodies with a recognizable dendritic tree or axonal projection remaining within a given cerebellar lobule. The data were expressed as the number of Purkinje cells per 100 μm of Purkinje cell layer: granule cell layer interface. The whole cerebellar area or individual cerebellar lobules were manually identified from the Hoechst 33342 channel images (DNA counterstain) using the default region of interest function of ImageJ.

Statistical analysis

Statistical comparisons were performed using GraphPad Prism 5 software (San Diego, CA, USA). Box and whisker plots display the Tukey method, and direct comparison between 2 groups was performed using the Mann-Whitney test. For experiments using multiple concentrations of a drug, significance was assessed using Kruskal-Wallis One-way ANOVA. For the lifespan estimation, data were plotted in Kaplan-Meier survival curves, using the log rank test for survival analysis, plotting percent survival as a function of time in days. Results were considered significant if the p- value was <0.05. Figures and Tables were created in Microsoft office 2016 (Redmond, WA, USA).

Results

EAAT1/*Slc1a3* cerebellar expression and function

Although *Slc1a3* expression is not significantly reduced in cerebellar lobules from *Npc1*$^{-/-}$ mice (Fig. 1a) [11], single cell transcriptome analysis showed *Slc1a3* expression was significantly decreased in *Npc1*$^{-/-}$ cerebellar astrocytes (Fig. 1b)[20]. Western blot analysis confirmed decreased EAAT1 protein expression in cerebellar tissue from *Npc1*$^{-/-}$ mice (Fig. 2a) and NPC1 patients (Fig. 2b), suggesting that EAAT1 dysregulation may contribute to both mouse and human pathology. In the cerebellum, EAAT1 is expressed primarily by astrocytes. Decreased surface expression of EAAT1 protein on *Npc1*$^{-/-}$ astrocytes was measured by flow cytometry analysis of cells from mechanically disassociated cerebellar tissue and of cultured astrocytes (Fig. 2c). To assess if the decreased expression of EAAT1 by *Npc1*$^{-/-}$ astrocytes had functional consequences, we measured glutamate uptake. In comparison to *Npc1*$^{+/+}$ astrocytes, cultured *Npc1*$^{-/-}$ astrocytes deplete exogenous glutamate from the culture medium at a significantly slower rate at 3 ($p<0.05$) and 6 ($p<0.01$, two-way ANOVA) hours (Fig. 2d). Decreased expression of EAAT1 protein and functional impairment of glutamate uptake by *Npc1*$^{-/-}$ astrocytes, is consistent with the hypothesis that glutamate-mediated neurotoxicity contributes to NPC1 neuropathology.

In vitro stimulation of astrocyte glutamate uptake

We evaluated the potential of candidate therapeutic agents to increase glutamate uptake in *Npc1*$^{-/-}$ astrocytes using an in vitro assay. Miglustat and 2-hydroxypropyl-β-cyclodextrin (HPβCD, Kleptose HPB) are two drugs that have been shown to be effective in reducing neurological disease progression in animal models [29–31] and in NPC1 patients [32]. Glutamate uptake significantly decreased by 30% in *Npc1*$^{-/-}$ astrocytes ($p<0.01$) relative to *Npc1+/+* astrocytes (Fig. 2e). Exposure of *Npc1*$^{-/-}$ astrocytes to 100μM miglustat increased glutamate uptake from 70% to 92% of control levels ($p=0.07$); whereas exposure to 100μM HPβCD increased ($p<0.005$) glutamate uptake to 97% of control (Fig. 2e). These data suggest that drugs which decrease endolysosomal glycosphingolipid (miglustat) or unesterified cholesterol (HPβCD) improve glutamate uptake by *Npc1* mutant astrocytes.

Using this in vitro assay system, we also evaluated two drugs, ceftriaxone and riluzole, which directly modulate glutamate uptake, a therapeutic approach that has not been studied in NPC1. In addition to EAAT1, astrocytes also express EAAT2 (GLT-1) which, although less prominent in the cerebellum, is the major glutamate transporter in the brain [33]. EAAT2 is encoded for by *SLC1A2*. In a high throughput screen of FDA-approved drugs Rothstein *et al.* [34] found that beta-lactam antibiotics stimulate *SLC1A2* expression, and that ceftriaxone increased both gene and protein expression in vivo. We thus tested whether ceftriaxone, a brain penetrant β-lactam, could increase glutamate uptake in *Npc1*$^{-/-}$ astrocytes. Mean glutamate uptake was increased in a dose dependent manner ($p<0.05$, Kruskal-Wallis One-way ANOVA) to 84% and 102% of control levels when *Npc1*$^{-/-}$ astrocytes were exposed overnight to either 10 or 100μM ceftriaxone, respectively (Fig. 2e). Riluzole (Rilutek) is a neuroprotective drug that has been approved by the FDA for the treatment of amyotrophic lateral sclerosis. Although the clinical mechanism of action has not been definitively established, riluzole may decrease glutamate neurotoxicity by both inhibiting the presynaptic release of glutamate and noncompetitive inhibition of NMDA receptors [35]. Riluzole has also been shown to increase glutamate uptake by glutamate transporters including EAAT2 and EAAT1 [36–38]. We thus tested the ability of riluzole to increase glutamate uptake by *Npc1*$^{-/-}$ cerebellar astrocytes. Although the vehicle, DMSO, has been reported to have a beneficial effect on the *Npc1*$^{-/-}$ cellular phenotype [39], the increase in glutamate uptake in DMSO-treated compared to PBS-treated *Npc1*$^{-/-}$ astrocytes was not significant ($p=0.13$). Using the in vitro assay, we observed a dose-dependent restoration ($p<0.005$, Kruskal-Wallis One-way ANOVA) of glutamate uptake to 74%, 82% and 107% of control levels for 1, 10 and 100μM riluzole, respectively (Fig. 2e).

In vivo efficacy of ceftriaxone

Based on our in vitro study we investigated the potential efficacy of ceftriaxone in vivo. Ceftriaxone (100mg.kg^{-1} (n=14) or vehicle (PBS, n=15)) was administered daily to NPC1 mutant mice by intraperitoneal injection. Treatment of *Npc1*$^{-/-}$ mice with ceftriaxone did not delay neurological progression (Fig. 3a) or extend lifespan (Fig. 3b). Of note, throughout the treatment period, both control and mutant ceftriaxone treated mice developed diarrhea and had poor weight gain. This is a known side effect of antibiotic treatment and may have confounded survival data. However, histopathological evaluation showed no significant effect of ceftriaxone treatment on either microgliosis, astrogliosis or Purkinje neuron loss

at 7 weeks of age when comparing PBS and ceftriaxone treated *Npc1*$^{-/-}$ cerebellar tissue (Figs. 3c–e and S1a). In addition, the expression of both *Slc1a2* and *Slc1a3* was increased in response to ceftriaxone treatment in cerebellar tissue from *Npc1*$^{+/+}$ mice. In contrast, only *Slc1a2* expression was increased in *Npc1*$^{-/-}$ mice, whereas *Slc1a3* expression was unchanged (Fig. S1b). These data suggest a differential expression pattern for *Slc1a3* in the *Npc1*$^{-/-}$ cerebellum. Consistent with the histopathological result, *Gfap* expression showed only a trend (p=0.07) toward being decreased in ceftriaxone treated mice (Fig. S1b).

Riluzole delays neurological disease progression in *Npc1*$^{-/-}$ mice

Based on our in vitro data, we also evaluated the therapeutic potential of riluzole to treat NPC1. To test this, we treated *Npc1*$^{-/-}$ mice with 60μg.ml^{-1} riluzole added to the drinking water starting at 3 weeks of age. Analysis of cerebellar tissue from 7-week-old mice confirmed that riluzole increased expression of *Slc1a3* by 2.1- and 1.7-fold over vehicle control levels in *Npc1*$^{+/+}$ (p=0.005) and *Npc1*$^{-/-}$ mice (p=0.002), respectively (Fig. S2b). Histopathological evaluation of cerebellar tissue showed that riluzole did not decrease microglial activation characterized by CD68+ staining, but significantly (p<0.001) decreased astrogliosis as characterized by GFAP+ staining (Fig. 4 c,d and Fig. S2b). Treatment with riluzole also resulted in preservation of Calbindin D positive Purkinje neurons (Figs. 4e and S2a). Consistent with improved histopathology, we observed that riluzole treatment (n=13) delayed NPC1 disease progression (Fig. 4a) and significantly (p=0.02) increased survival compared to vehicle (DMSO, n=20) treated *Npc1*$^{-/-}$ mice (Fig. 4b). Median survival was increased 12% from 73 to 82 days. 2-hydroxypropyl-β-cyclodextrin (HPβCD) has been shown to significantly increase survival of *Npc1*$^{-/-}$ mice, thus we explored whether combined riluzole/HPβCD therapy would be of benefit. No significant (p=0.63) survival difference was observed comparing HPβCD (median 106 days, n=13) and HPβCD + riluzole (median 108 days, n=12) treatment (Fig. 4b).

Discussion

Glutamate mediated excitotoxicity has been proposed to be a pathological mechanism contributing to neurodegeneration in multiple disorders including amyotrophic lateral sclerosis, Huntington disease and Alzheimer disease [23]. We previously noted decreased *Slc1a3* expression in cerebellar astrocytes from *Npc1*$^{-/-}$ mice [20]. These data were consistent with work by Rabenstein *et al.* [21] who showed reduced protein levels of EAAT1, EAAT2 and EAAT4 in cerebellar tissue from *Npc1*$^{-/-}$ mice. Based on these results we considered that the reduced levels of these glutamate transporters contribute to glutamate-mediated excitotoxicity and neurodegeneration in NPC1. We hypothesized that increasing their level and function would have a beneficial effect in treating NPC1. To test this hypothesis, we evaluated the therapeutic benefit of both ceftriaxone and riluzole in *Npc1*$^{-/-}$ mice.

Ceftriaxone is a beta-lactam antibiotic that has been shown to increase *Slc1a2* expression and corresponding EAAT2 activity *in vivo* [34]. Although ceftriaxone treatment of *Npc1*$^{+/+}$ and *Npc1*$^{-/-}$ mice increased expression of *Slc1a2*, we did not observe any histopathological, phenotypic or survival benefit in ceftriaxone treated NPC1 mutant mice. There are several

possible explanations for this negative result. EAAT2 is the major glutamate transporter in the brain; however, it plays less of a role in the cerebellum where EAAT1 plays a major role [33]. Thus, upregulation of EAAT2 may be less effective for disorders such as NPC1 where cerebellar Purkinje neuron loss is a major pathological feature. Our data also show that ceftriaxone induced expression of *Slc1a2* appears to be blunted in the NPC1 mutant cerebellar tissue relative to controls. Ceftriaxone induced expression of *Slc1a2* is mediated by an NFκB binding site [40], thus it is possible that the prominent neuroinflammation and neurodegeneration in the mutant mouse cerebellar tissue alters NFκB signaling. Alternatively, although we confirmed that ceftriaxone increased glutamate uptake by $Npc1^{-/-}$ astrocytes in vitro and observed increased, but blunted, *Slc1a2* expression in cerebellar tissue from treated mice, we did not establish a corresponding increase in expression of EAAT2 protein. We did observe increased expression of *Slc1a3* in cerebellar tissue from ceftriaxone treated $Npc1^{+/+}$ mice. This contrasts with a lack of increased EAAT1 protein in hippocampal tissue from ceftriaxone treated mice [34]. To our knowledge this observation has not been previously reported; however, given that we did not observe increased expression of *Slc1a3* in the $Npc1^{-/-}$ mutant mice, this observation was not pursued further in the context of this study.

Riluzole is a neuroprotective drug which inhibits the release of presynaptic glutamate and facilitates glutamate uptake by excitatory amino acid transporters [35, 41] and riluzole has been shown to protect Purkinje neurons in a rat model of cerebellar ataxia [42]. Riluzole has been approved by the FDA for the treatment of amyotrophic lateral sclerosis and has been studied in children with obsessive compulsive disorder [43]. This raises the possibility that riluzole could be repurposed for the treatment of individuals with NPC1. In this study we found that treatment of $Npc1^{-/-}$ mice with riluzole decreased astrogliosis, delayed Purkinje neuron loss, improved the neurological phenotype and increased survival. The histopathological analysis is notable in that riluzole did not appear to impact neuroinflammation which occurs early in the disease [11, 20, 26], but rather had a more pronounced effect on astrogliosis which appears to occur later in the NPC1 pathological cascade [44]. Indeed, the disease severity score began to diverge after 8 weeks (Fig. 4a) as reduced disease severity scores were observed in the treated mice. This is coincidental with the timing of increased astrogliosis during normal disease progression and suggests a reduced progression of the disease in the riluzole treated mice due to the reduced astrogliosis. This apparent later effect of riluzole on the NPC1 pathological cascade may explain the lack of an observed benefit when combined with HPβCD. HPβCD has been shown to have very early effects on NPC1 histopathology. In this paper we only explored the potential of riluzole to complement an optimized dose of HPβCD initiated in presymptomatic animals. These data do not exclude the possibility that this drug combination could show benefit under other experimental paradigms. The observation that riluzole appears to have more of an impact on astrogliosis also suggests that combining riluzole with an anti-inflammatory drug which suppresses microgliosis may be of benefit.

We postulate that the beneficial effect of riluzole in $Npc1^{-/-}$ mice is due to decreased glutamate-mediated neurotoxicity. This conclusion is based on riluzole's reported mechanism of action, increased in vitro glutamate uptake by $Npc1^{-/-}$ astrocytes treated with riluzole and increased expression of *Slc1a3* in cerebellar tissue from riluzole treated $Npc1^{-/-}$

mice. In addition to the work presented in this paper, multiple studies suggest a disturbance of glutamate signaling in *Npc1* mutant mice. Analogous to our finding of decreased cerebellar astrocyte EAAT1 protein expression, Byun et al. [45] reported decreased protein expression of EAAT3 (EAAC1, SLC1A1) in hippocampal tissue from $Npc1^{-/-}$ mice. Work by both D'Arcangelo *et al.* [46] and Feng *et al.* [47] indicate impaired AMPA receptor internalization. These observations provide additional evidence of impaired glutamate homeostasis in NPC1 and support our conclusion that glutamate-mediated neurotoxicity contributes to NPC1 neuropathology.

Conclusions

The data reported in this paper support the conclusion that glutamate mediated neurotoxicity likely contributes to NPC1 neuropathology and demonstrate that treatment with riluzole has beneficial effects in the NPC1 mouse model. Given that riluzole is an approved drug for the treatment of amyotrophic lateral sclerosis, repurposing of this drug, or use of other agents which reduce glutamate-mediated neurotoxicity, may provide a novel therapeutic approach to decrease disease progression in Niemann-Pick disease type C1 patients.

Supplementary Material

Refer to Web version on PubMed Central for supplementary material.

Acknowledgements

Not applicable

Funding

This work was supported by the intramural research program of the *Eunice Kennedy Shriver* National Institute of Child Health and Human Development, National Institutes of Health. This work was also supported by a grant from the Ara Parseghian Medical Research Foundation.

List of Abbreviations

CALB	Calbindin
CTX	Ceftriaxone
DMSO	Dimethyl Sulfoxide
EAAT	Excitatory Amino Acid Transporters
FDA	Federal Drug Administration
GFAP	Glial Fibrillary Acidic Protein
HPβCD	2-hydroxypropyl-β-cyclodextrin
MFI	Mean Fluorescent Intensity
NICHD	*Eunice Kennedy Shriver* National Institute of Child Health and Human Development

NPC	Niemann-Pick Disease, type C
NPC1	Niemann-Pick Disease, type C1
NPC2	Niemann-Pick Disease, type C2
PBS	Phosphate Buffered Saline

References

1. Vanier MT, Niemann-Pick disease type C. Orphanet J Rare Dis, 2010. 5: p. 16. [PubMed: 20525256]
2. Wassif CA, et al. , High incidence of unrecognized visceral/neurological late-onset Niemann-Pick disease, type C1, predicted by analysis of massively parallel sequencing data sets. Genet Med, 2016. 18(1): p. 41–8. [PubMed: 25764212]
3. Pfeffer SR, NPC intracellular cholesterol transporter 1 (NPC1)-mediated cholesterol export from lysosomes. J Biol Chem, 2019. 294(5): p. 1706–1709. [PubMed: 30710017]
4. Crocker AC and Farber S, Niemann-Pick disease: a review of eighteen patients. Medicine (Baltimore), 1958. 37(1): p. 1–95. [PubMed: 13516139]
5. Bianconi SE, et al. , Evaluation of age of death in Niemann-Pick disease, type C: Utility of disease support group websites to understand natural history. Mol Genet Metab, 2019. 126(4): p. 466–469. [PubMed: 30850267]
6. Patterson MC, et al. , Long-term survival outcomes of patients with Niemann-Pick disease type C receiving miglustat treatment: A large retrospective observational study. J Inherit Metab Dis, 2020.
7. Patterson MC, et al. , Treatment outcomes following continuous miglustat therapy in patients with Niemann-Pick disease Type C: a final report of the NPC Registry. Orphanet J Rare Dis, 2020. 15(1): p. 104. [PubMed: 32334605]
8. Solomon BI, et al. , Association of Miglustat With Swallowing Outcomes in Niemann-Pick Disease, Type C1. JAMA Neurol, 2020.
9. Sarna JR and Hawkes R, Patterned Purkinje cell death in the cerebellum. Prog Neurobiol, 2003. 70(6): p. 473–507. [PubMed: 14568361]
10. Higashi Y, et al. , Cerebellar degeneration in the Niemann-Pick type C mouse. Acta Neuropathol, 1993. 85(2): p. 175–84. [PubMed: 8382896]
11. Martin KB, et al. , Identification of Novel Pathways Associated with Patterned Cerebellar Purkinje Neuron Degeneration in Niemann-Pick Disease, Type C1. Int J Mol Sci, 2019. 21(1).
12. Perkins EM, et al. , Loss of cerebellar glutamate transporters EAAT4 and GLAST differentially affects the spontaneous firing pattern and survival of Purkinje cells. Hum Mol Genet, 2018. 27(15): p. 2614–2627. [PubMed: 29741614]
13. Slemmer JE, De Zeeuw CI, and Weber JT, Don't get too excited: mechanisms of glutamate-mediated Purkinje cell death. Prog Brain Res, 2005. 148: p. 367–90. [PubMed: 15661204]
14. Miyazaki T, et al. , Glutamate transporter GLAST controls synaptic wrapping by Bergmann glia and ensures proper wiring of Purkinje cells. Proc Natl Acad Sci U S A, 2017. 114(28): p. 7438–7443. [PubMed: 28655840]
15. Nagao S, Kwak S, and Kanazawa I, EAAT4, a glutamate transporter with properties of a chloride channel, is predominantly localized in Purkinje cell dendrites, and forms parasagittal compartments in rat cerebellum. Neuroscience, 1997. 78(4): p. 929–33. [PubMed: 9174061]
16. Farooqui AA and Horrocks LA, Involvement of glutamate receptors, lipases, and phospholipases in long-term potentiation and neurodegeneration. J Neurosci Res, 1994. 38(1): p. 6–11. [PubMed: 8057391]
17. Lau A and Tymianski M, Glutamate receptors, neurotoxicity and neurodegeneration. Pflugers Arch, 2010. 460(2): p. 525–42. [PubMed: 20229265]
18. Arriza JL, et al. , Functional comparisons of three glutamate transporter subtypes cloned from human motor cortex. J Neurosci, 1994. 14(9): p. 5559–69. [PubMed: 7521911]

19. Martinez-Lozada Z, Guillem AM, and Robinson MB, Transcriptional Regulation of Glutamate Transporters: From Extracellular Signals to Transcription Factors. Adv Pharmacol, 2016. 76: p. 103–45. [PubMed: 27288076]
20. Cougnoux A, et al. , Single Cell Transcriptome Analysis of Niemann-Pick Disease, Type C1 Cerebella. Int J Mol Sci, 2020. 21(15).
21. Rabenstein M, et al. , Impact of Reduced Cerebellar EAAT Expression on Purkinje Cell Firing Pattern of NPC1-deficient Mice. Sci Rep, 2018. 8(1): p. 3318. [PubMed: 29463856]
22. Choi KD, et al. , Late-onset episodic ataxia associated with SLC1A3 mutation. J Hum Genet, 2017. 62(3): p. 443–446. [PubMed: 27829685]
23. Lewerenz J and Maher P, Chronic Glutamate Toxicity in Neurodegenerative Diseases-What is the Evidence? Front Neurosci, 2015. 9: p. 469. [PubMed: 26733784]
24. Loftus SK, et al. , Murine model of Niemann-Pick C disease: mutation in a cholesterol homeostasis gene. Science, 1997. 277(5323): p. 232–5. [PubMed: 9211850]
25. Guyenet SJ, et al. , A simple composite phenotype scoring system for evaluating mouse models of cerebellar ataxia. J Vis Exp, 2010(39).
26. Cougnoux A, et al. , Microglia activation in Niemann-Pick disease, type C1 is amendable to therapeutic intervention. Hum Mol Genet, 2018. 27(12): p. 2076–2089. [PubMed: 29617956]
27. Schindelin J, et al. , Fiji: an open-source platform for biological-image analysis. Nat Methods, 2012. 9(7): p. 676–82. [PubMed: 22743772]
28. Cougnoux A, et al. , Necroptosis inhibition as a therapy for Niemann-Pick disease, type C1: Inhibition of RIP kinases and combination therapy with 2-hydroxypropyl-beta-cyclodextrin. Mol Genet Metab, 2018. 125(4): p. 345–350. [PubMed: 30392741]
29. Davidson CD, et al. , Chronic cyclodextrin treatment of murine Niemann-Pick C disease ameliorates neuronal cholesterol and glycosphingolipid storage and disease progression. PLoS One, 2009. 4(9): p. e6951. [PubMed: 19750228]
30. Liu B, et al. , Reversal of defective lysosomal transport in NPC disease ameliorates liver dysfunction and neurodegeneration in the npc1−/− mouse. Proc Natl Acad Sci U S A, 2009. 106(7): p. 2377–82. [PubMed: 19171898]
31. Vite CH, et al. , Intracisternal cyclodextrin prevents cerebellar dysfunction and Purkinje cell death in feline Niemann-Pick type C1 disease. Sci Transl Med, 2015. 7(276): p. 276ra26.
32. Ory DS, et al. , Intrathecal 2-hydroxypropyl-beta-cyclodextrin decreases neurological disease progression in Niemann-Pick disease, type C1: a non-randomised, open-label, phase 1–2 trial. Lancet, 2017. 390(10104): p. 1758–1768. [PubMed: 28803710]
33. Kim K, et al. , Role of excitatory amino acid transporter-2 (EAAT2) and glutamate in neurodegeneration: opportunities for developing novel therapeutics. J Cell Physiol, 2011. 226(10): p. 2484–93. [PubMed: 21792905]
34. Rothstein JD, et al. , Beta-lactam antibiotics offer neuroprotection by increasing glutamate transporter expression. Nature, 2005. 433(7021): p. 73–7. [PubMed: 15635412]
35. Doble A, The pharmacology and mechanism of action of riluzole. Neurology, 1996. 47(6 Suppl 4): p. S233–41. [PubMed: 8959995]
36. Fumagalli E, et al. , Riluzole enhances the activity of glutamate transporters GLAST, GLT1 and EAAC1. Eur J Pharmacol, 2008. 578(2–3): p. 171–6. [PubMed: 18036519]
37. Carbone M, Duty S, and Rattray M, Riluzole elevates GLT-1 activity and levels in striatal astrocytes. Neurochem Int, 2012. 60(1): p. 31–8. [PubMed: 22080156]
38. Dall'Igna OP, et al. , Riluzole increases glutamate uptake by cultured C6 astroglial cells. Int J Dev Neurosci, 2013. 31(7): p. 482–6. [PubMed: 23777615]
39. Blanchette Mackie EJ, et al. , Type C Niemann-Pick disease: dimethyl sulfoxide moderates abnormal LDL-cholesterol processing in mutant fibroblasts. Biochim Biophys Acta, 1989. 1006(2): p. 219–26. [PubMed: 2688743]
40. Lee SG, et al. , Mechanism of ceftriaxone induction of excitatory amino acid transporter-2 expression and glutamate uptake in primary human astrocytes. J Biol Chem, 2008. 283(19): p. 13116–23. [PubMed: 18326497]

41. Azbill RD, Mu X, and Springer JE, Riluzole increases high-affinity glutamate uptake in rat spinal cord synaptosomes. Brain Res, 2000. 871(2): p. 175–80. [PubMed: 10899284]

42. Janahmadi M, et al. , Co-treatment with riluzole, a neuroprotective drug, ameliorates the 3-acetylpyridine-induced neurotoxicity in cerebellar Purkinje neurones of rats: behavioural and electrophysiological evidence. Neurotoxicology, 2009. 30(3): p. 393–402. [PubMed: 19442824]

43. Grant P, et al. , Riluzole Serum Concentration in Pediatric Patients Treated for Obsessive-Compulsive Disorder. J Clin Psychopharmacol, 2017. 37(6): p. 713–716. [PubMed: 29045303]

44. Pressey SN, et al. , Early glial activation, synaptic changes and axonal pathology in the thalamocortical system of Niemann-Pick type C1 mice. Neurobiol Dis, 2012. 45(3): p. 1086–100. [PubMed: 22198570]

45. Byun K, et al. , Alteration of the glutamate and GABA transporters in the hippocampus of the Niemann-Pick disease, type C mouse using proteomic analysis. Proteomics, 2006. 6(4): p. 1230–6. [PubMed: 16429462]

46. D'Arcangelo G, et al. , Glutamatergic neurotransmission in a mouse model of Niemann-Pick type C disease. Brain Res, 2011. 1396: p. 11–9. [PubMed: 21575932]

47. Feng X, et al. , Stimulation of mGluR1/5 Improves Defective Internalization of AMPA Receptors in NPC1 Mutant Mouse. Cereb Cortex, 2020. 30(3): p. 1465–1480. [PubMed: 31599924]

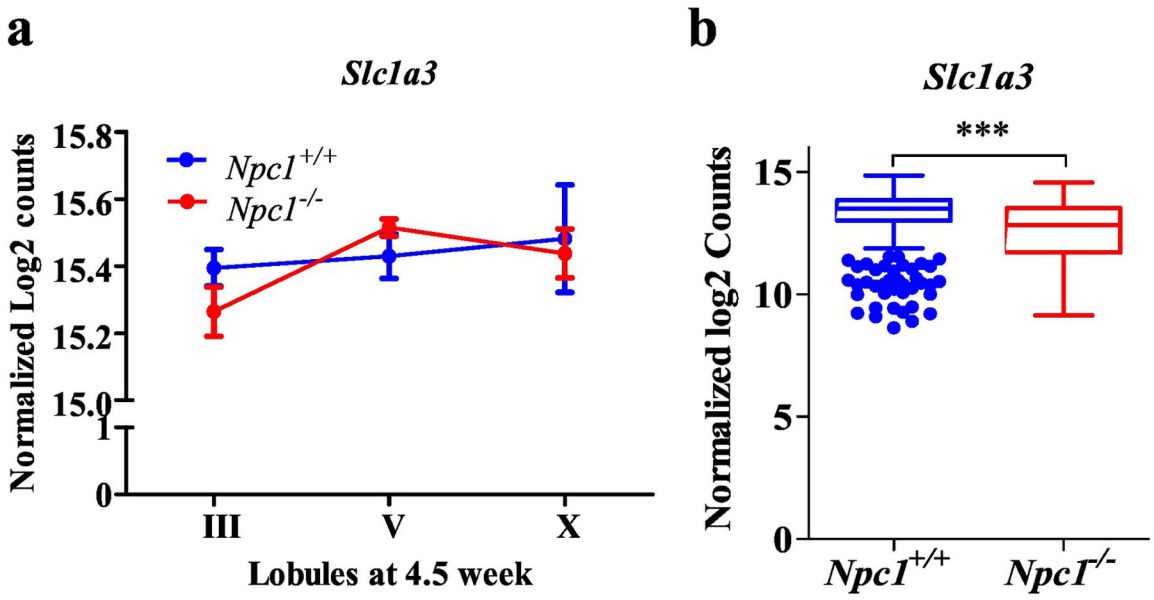

Figure 1.

Slc1a3 normalized expression derived from our previously published datasets investigating transcriptional changes in *Npc1*$^{-/-}$ mouse cerebellar lobules **(a)** at 4.5 weeks of age [11] (https://porterlab.shinyapps.io/cerebellarlobules/), and by single cell transcriptome analysis **(b)** of astrocytes from *Npc1*$^{+/+}$ (n=435) and *Npc1*$^{-/-}$ (n=226) mouse cerebellar tissue at 7 weeks of age (SRA accession number: PRJNA606815) [20]. *Npc1*$^{+/+}$ (blue). *Npc1*$^{-/-}$ (red). ***p<0.001

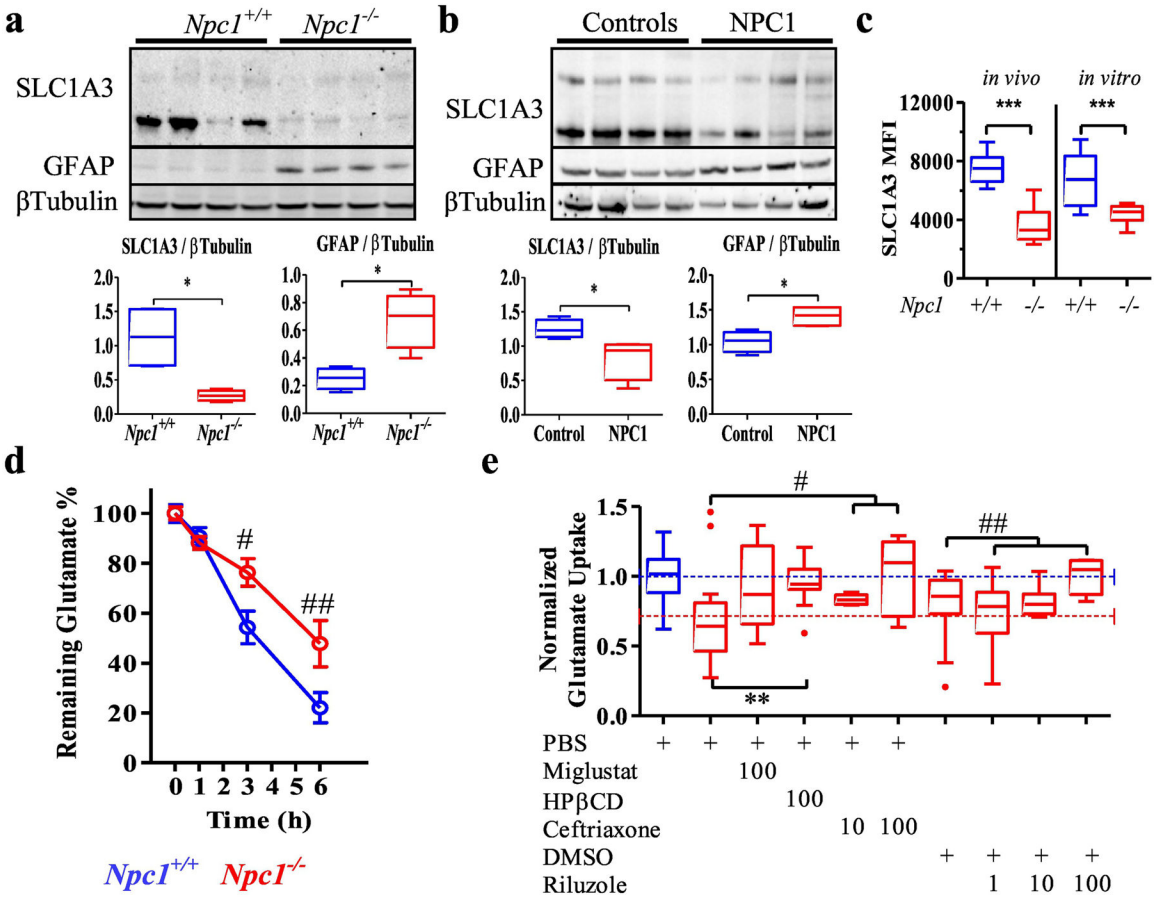

Figure 2.

SLC1A3 dysregulation in Niemann-Pick type C. **a** Western blot analysis of SLC1A3, GFAP and βTubulin expression in 7-week-old mouse cerebellar extracts and densitometric quantification. N=4. **b** Western blot analysis of SLC1A3, GFAP and βTubulin expression in NPC1 and control human cerebellar extracts and densitometric quantification. N=4 **c** SLC1A3 surface expression level (Mean Fluorescence Intensity) on astrocytes isolated from 7-week-old cerebellar tissue (*in vivo*) or primary cerebellar astrocytes cultured (in vitro) from *Npc1*$^{+/+}$ and *Npc1*$^{-/-}$ mice. **d** Decrease in glutamate levels in the culture media from *Npc1*$^{+/+}$ and *Npc1*$^{-/-}$ primary astrocytes. **e** Tukey box and whisker plot of glutamate uptake from culture media was significantly (p<0.01) reduced in *Npc1*$^{-/-}$ astrocytes compared to uptake by *Npc1*$^{+/+}$ astrocytes. Data was normalized to *Npc1*$^{+/+}$ uptake. The average values for *Npc1*$^{+/+}$ (blue) and *Npc1*$^{-/-}$ (red) are indicated by dashed lines. Glutamate uptake by *Npc1*$^{-/-}$ astrocytes was increased by treatment with miglustat (p=0.07), HPβCD (p<0.005), ceftriaxone (p<0.05) or riluzole (p<0.005). PBS was the vehicle for miglustat, HPβCD and ceftriaxone. DMSO was the vehicle for riluzole. Drug concentrations are in micromolar. *Npc1*$^{+/+}$ (blue), *Npc1*$^{-/-}$ (red). *p<0.05, **p<0.01 and ***p<0.001 Mann-Whitney, #p<0.05 and ##p<0.01 ANOVA.

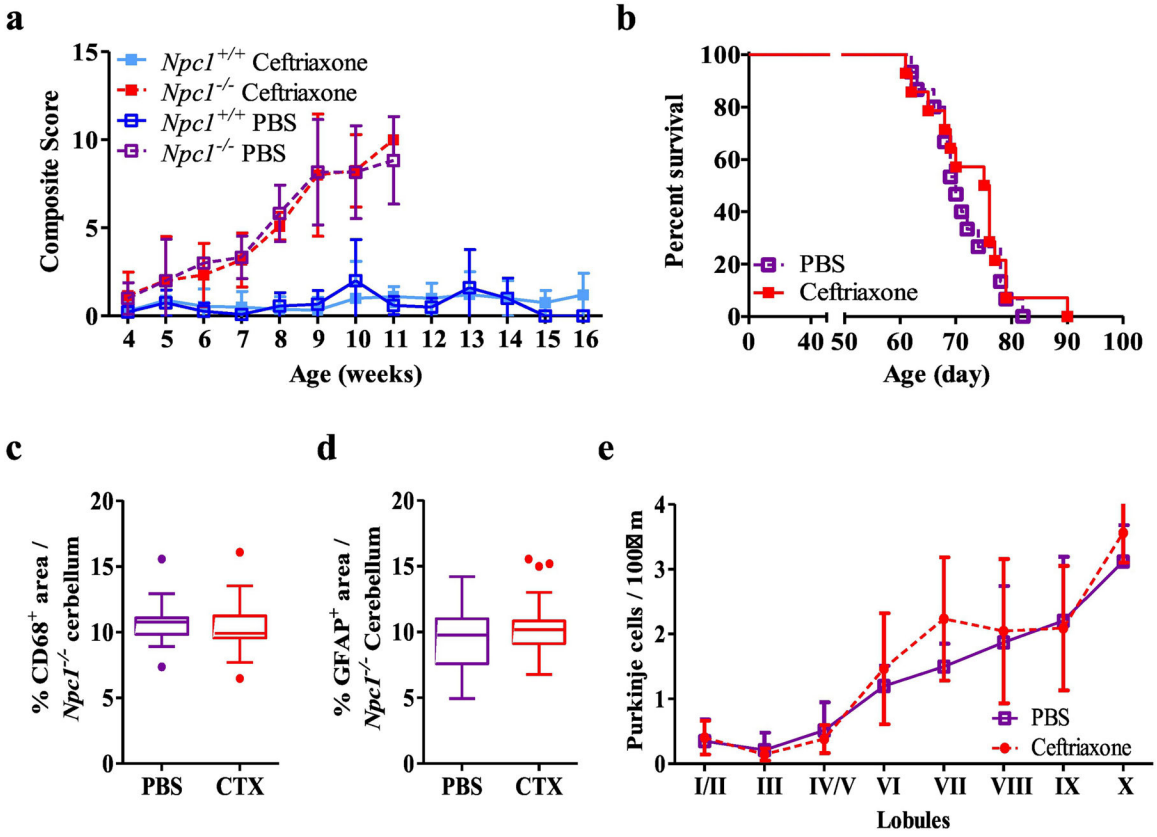

Figure 3.

In vivo evaluation of ceftriaxone. **a** NPC1 disease composite score evaluation between 4 and 16 weeks for vehicle (PBS, initial n=9 and 23) and ceftriaxone (100 mg.kg^{-1}, initial n=13 and 15) treated *Npc1*$^{-/-}$ and *Npc1*$^{+/+}$ mice. Initial n values are for *Npc1*$^{-/-}$ and *Npc1*$^{+/+}$ respectively). These numbers become truncated as the experiment progresses. **b** Kaplan-Meier survival analysis of PBS (n=15) and ceftriaxone (n=14) treated *Npc1*$^{-/-}$ mice. **c** Immunofluorescence quantification of CD68 in cerebellar tissue from 7-week-old PBS or ceftriaxone treated *Npc1*$^{-/-}$ mice. **d** Immunofluorescence quantification of GFAP in cerebellar tissue from 7-week-old PBS or ceftriaxone treated *Npc1*$^{-/-}$ mice. **e** Cerebellar lobule Purkinje neuron density per 100μm in 7-week-old of PBS or ceftriaxone treated *Npc1*$^{-/-}$ mice. Purkinje neurons were identified by immunostaining for calbindin. N≥6, *Npc1*$^{-/-}$ PBS (purple), *Npc1*$^{-/-}$ ceftriaxone (red), *Npc1*$^{+/+}$ PBS (dark blue), *Npc1*$^{+/+}$ ceftriaxone (light blue).

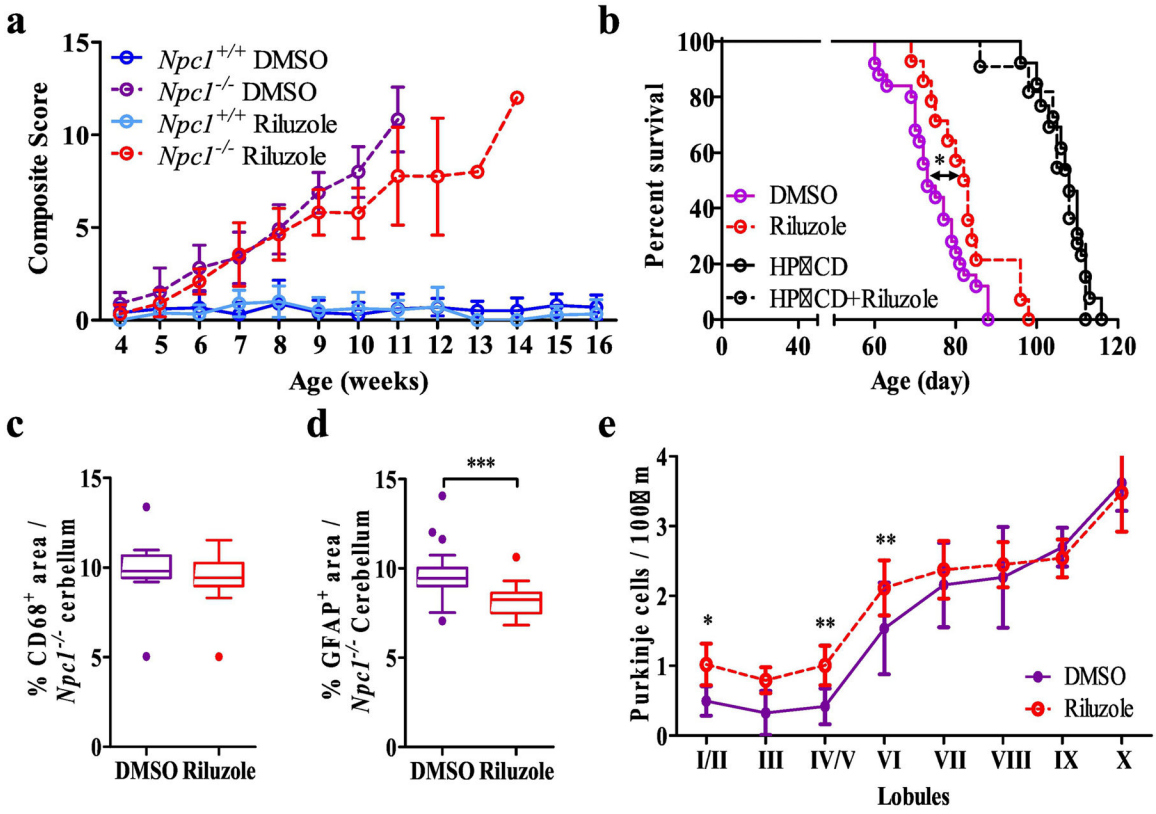

Figure 4.

In vivo evaluation of riluzole. **a** NPC1 disease composite score evaluation between 4 and 16 weeks of age with DMSO (initial n=16 and 14) and riluzole treated (60µg.ml^{-1} in the drinking water, initial n=12 and 18) *Npc1*$^{-/-}$ and *Npc1*$^{+/+}$ mice. Initial n values are for *Npc1*$^{-/-}$ and *Npc1*$^{+/+}$ respectively). These numbers become truncated as the experiment progresses. **b** Kaplan-Meier survival analysis of DMSO (n=20), riluzole (n=14), HPβCD (n=13) and HPβCD + riluzole (n=12) treated *Npc1*$^{-/-}$ mice. **c** Immunofluorescence quantification of cerebellar CD68 staining in 7-week-old of DMSO or riluzole treated *Npc1*$^{-/-}$ mice. **d** Immunofluorescence quantification of cerebellar GFAP staining in 7-week-old of DMSO or riluzole treated *Npc1*$^{-/-}$ mice. **e** Cerebellar lobule Purkinje cell density per 100µm in 7-week-old of PBS or ceftriaxone treated *Npc1*$^{-/-}$ mice. Purkinje neurons were identified by immunostaining for calbindin. N≥6, *Npc1*$^{-/-}$ DMSO (purple), *Npc1*$^{-/-}$ riluzole (red), *Npc1*$^{+/+}$ DMSO (blue), *Npc1*$^{+/+}$ Riluzole (light blue). *p<0.05, **p<0.01 and ***p<0.001.